

New Vanadium, Titanium and Yttrium PNP Pincer Complexes based on 2,6-Diaminopyridine

Rita Alvarez Ruivo

Instituto Superior Técnico, Universidade de Lisboa, Av. Rovisco Pais 1, 1049-001 Lisboa, Portugal

ABSTRACT

The synthesis of transition metal complexes (Ti^{III}, V^{III} and Y^{III}) based on 2,6-diaminopyridine PNP ligands is reported. Vanadium complexes of formulas [V(PNP-ⁱPr₂)Cl₃], [V(PNP-Ph₂)Cl₃], [V(PNP^{Me}-ⁱPr₂)Cl₃] and [Ti(PNP-Ph₂)Cl₃] were characterized by infrared spectroscopy, elemental analysis and X-ray crystallography. The complex [V(PNP-Ph₂)Cl₃] was also prepared without solvent through mechanochemistry. The Yttrium complex [Y(PNP)Cl₂][YCl₄] was characterized by infrared spectroscopy, elemental analysis and ESI-MS. Titanium and Yttrium PNP pincer complexes are described here for the first time.

Keywords: Vanadium complexes; Titanium complexes; Yttrium complexes; Pincer ligands; PNP pincer.

1. Introduction

Among the many ligand systems that can be found in the chemical literature, pincer ligands play an important role and their complexes have attracted tremendous interest due to their high stability and activity^[1]. These tridentate ligands are planar scaffolds consisting of a neutral central pyridine backbone tethered to two, mostly bulky, two-electron donor groups by different spacers. In this family of ligands, steric, electronic parameters can be manipulated by modifications of the substituents at the donor sites and/or the spacers. Many applications of mostly second and third row precious transition metal pincer complexes in the fields of catalysis and supramolecular chemistry were discovered, turning this area into an intensively investigated subject in organometallic chemistry^[2]. As non-precious transition metals are concerned, the

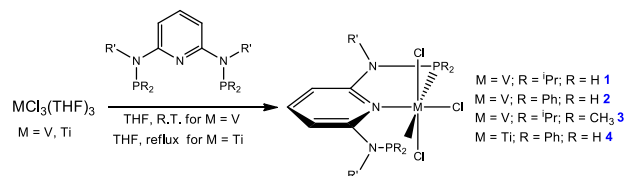
chemistry of neutral pyridine-based titanium and yttrium pincers appear to be unknown yet.

Herein is reported the synthesis, characterization and preliminary reactivity study of a series of new vanadium PNP complexes with the formulas [V(PNP-ⁱPr₂)Cl₃], [V(PNP-Ph₂)Cl₃] and [V(PNP^{Me}-ⁱPr₂)Cl₃]. Titanium and Yttrium PNP complexes, [Ti(PNP-Ph₂)Cl₃] and [Y(PNP-Ph)Cl₂][YCl₄], were also synthesized and characterized.

2. Results and Discussion

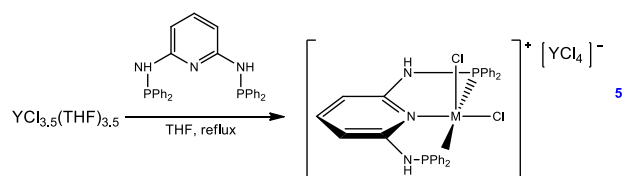
Treatment of [MCl₃(THF)₃] (M = V, Ti) with the suitable PNP ligands, PNP-ⁱPr, PNP-Ph, PNP^{Me}-ⁱPr in THF affords the six-coordinate 14e⁻ complexes [V(PNP-ⁱPr₂)Cl₃] (**1**), [V(PNP-Ph₂)Cl₃] (**2**) and [V(PNP^{Me}-ⁱPr₂)Cl₃] (**3**) and the 13e⁻ complex [Ti(PNP-

Ph₂)Cl₃] (**4**) in moderate yields of 72%, 60%, 68% and 54% respectively.



Scheme 1 - Synthesis of V^{III} complexes [V(PNP-ⁱPr₂)Cl₃], [V(PNP-Ph₂)Cl₃] and [V(PNP^{Me}-ⁱPr₂)Cl₃] and Ti^{III} [Ti(PNP-Ph₂)Cl₃].

Likewise, the reaction of the yttrium precursor, [YCl₃(THF)_{3.5}], with 2 equivalents of PNP-Ph ligand in THF afforded the cationic five-coordinate 11e⁻ complex [Y(PNP-Ph)Cl₂][YCl₄] (**5**) in 34% yield.



Scheme 2 - Synthesis of Y^{III} complex [Y(PNP-Ph)Cl₂][YCl₄].

Vanadium and Titanium complexes' ¹H, ³¹P{¹H} and ¹³C{¹H} NMR signals could not be obtained due to their paramagnetic nature. Yttrium complex ¹H and ¹³C{¹H} NMR spectra showed several overlapped resonances in the aromatic region attributed to the protons of the phenyl rings attached to the phosphines, the pyridine backbone and also the amino spacers of the PNP ligand. The ³¹P and ¹³C {¹H} NMR spectra is also not conclusive due to the presence of several peaks that might be attributed to the presence of two possible isomers of **5**. For these reasons, full NMR characterization of **5** was not possible.

Complexes **1**, **2** and **3** were characterized by IR spectroscopy. For compounds **1** and **2**, it is possible to find bands from 3400 to 3000 cm⁻¹ belonging to the

amine NH spacer and the pyridine backbone. The C-H stretching vibrations of the aromatic rings belonging to **2** can be found at 1964, 1891 and 1815 cm⁻¹. On the other hand, the aliphatic C-H stretching vibrations of the isopropyl group in **1** are found in the region from 3000-2700 cm⁻¹. For compound **3** the region from 2965 to 2873 cm⁻¹ shows bands belonging to the methyl amine spacer, the aliphatic C-H stretching vibrations of the isopropyl group and the pyridine backbone.

In complexes **1**, **2** and **3** the region from 1700 to 400 cm⁻¹ displays several bands belonging to different overlapped frequencies of the pyridine ring, the isopropyl group (in complex **1** and **3**), the phenyl group (in complex **2**) and the methyl amine spacer (complex **3**). When compared with the corresponding organic precursor spectra, the IR peaks of the three complexes appear at high frequencies.

The IR analysis of the titanium and yttrium complexes shows bands in the region between 3400 and 2900 cm⁻¹, belonging to the amine NH spacer, the pyridine backbone and the phenyl rings. **4**. However, complex **5** shows in the region of 3500 to 3100 cm⁻¹ a very intense broad band belonging to adventitious water.

It is possible to identify three bands belonging to the phenyl group attached to the phosphorous at 1961, 1890 and 1814 cm⁻¹ for the titanium complex and at 1961, 1893 and 1822 cm⁻¹ for the yttrium complex. The region of 1700 to 400 cm⁻¹ displays several overlapped bands belonging to different frequencies of the pyridine ring and the phenyl group, rendering single identification of the bands impossible.

The band shift observed between the organic precursor and the complexes' spectra constitutes a pattern identical to the one observed in the vanadium complexes.

Complexes **1**, **2** and **3** exhibit solution magnetic moments of 2.84, 2.56 and 2.86 Bohr Magnetons respectively, determined by the Evans method.^[3] The number of unpaired electrons considering spin-only moment contribution is consistent with the d^2 metal configuration of $2e$.

Acetonitrile solutions of **1**, **2** and **5** in the presence of NaCl were subject to ESI-MS analysis in the positive ion mode. In the case of V^{III} complexes **1** and **2**, the most abundant signals at m/z 443.38 and 597.12 correspond to an V^{III} species bearing an oxo ligand $[V(PNP-PR_2)ClO]^+$ highlighting the oxophilic characteristic of vanadium complexes. For complex **1** the species $[V(PNP-*i*Pr_2)Cl_2]^+$ was found at m/z 462.20 while for complex **2** $[V(PNP-Ph_2)Cl_2(2,6\text{-diaminopyridine})]^+$ was found at m/z 707.85. This result is consistent with the observations made by Kirchner and co-workers^[4], for iron PNP- Ph_2 complexes with the $-NH$ spacer, which undergo facile rearrangement reactions to give cationic complexes of the type $[Fe(\kappa^3\text{-P,N,P-PNP-Ph})(\kappa^2\text{-P,N-PNP-Ph})Cl]^+$. More sterically demanding ligands, such as PNP- i Pr₂ do not suffer this kind of rearrangement, originating complexes of the type $[Fe(\kappa^3\text{-P,N,P-PNP})Cl_2]$.

In the negative ion mode, the most abundant signals are observed at m/z equal to 534.11 **1** and 669.33 **2** which correspond to the anionic complexes $[V(PNP-PR_2)Cl_4]^-$. Signals at m/z of 498.13 **1** and 632.18 **2** correspond to the starting complexes with loss of a proton in the amino spacer $[V(PNP-PR_2)Cl_3]$.

For complex **5** the negative mode showed one evident signal at m/z 231.24 that corresponds to the $[YCl_4]^-$ fragment. This result is in accordance to the formulation performed by elemental analysis, suggesting the formation of a cationic complex of the type $[Y(PNP-Ph_2)Cl_2][YCl_4]$.

In order to unequivocally establish the ligand arrangement around the metal centres, the solid state structure of complexes **1**, **2**, **3** and **5** was determined by X-ray diffraction. ORTEP representations of these molecules are shown in Figures 1-4 with selected metrical parameters given in Tables 1 and 2.

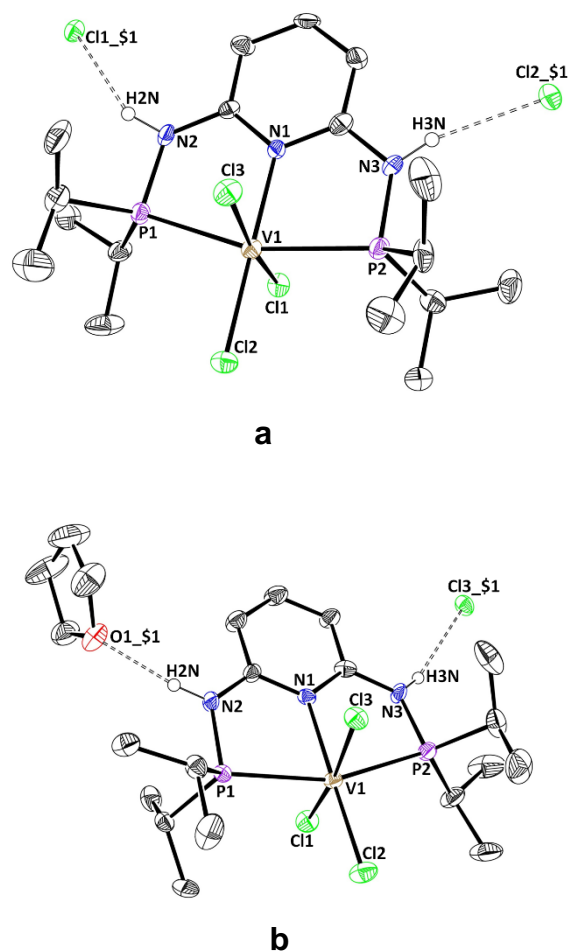


Figure 1 – Structural view of complex (**1**) $[V(PNP-*i*Pr_2)Cl_3]$ for two different solvomorphic structures in DCM (**a**) and THF (**b**), showing thermal ellipsoids at 40% probability level. In **1a** the hydrogen atoms and a co-crystallized DCM molecule are omitted for clarity. In **1b** the hydrogen atoms are omitted for clarity. Dashed lines represent hydrogen bonds.

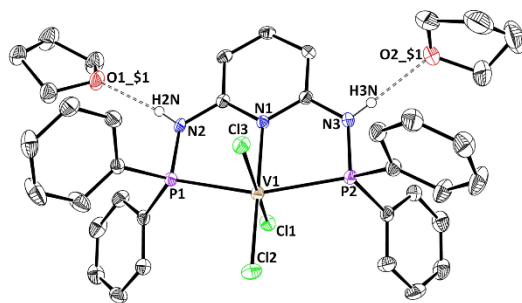


Figure 2 – Structural view of complex (2) [V(PNP-Ph₂)Cl₃] showing thermal ellipsoids at 40% probability level. The hydrogen atoms are omitted for clarity. Dashed lines represent hydrogen bonds.

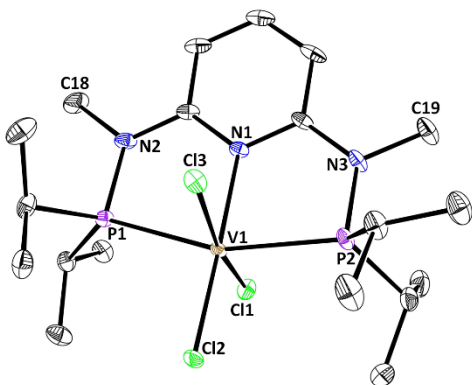


Figure 3 – Structural view of complex (3) [V(PNP^{Me}-iPr₂)Cl₃] showing thermal ellipsoids at 40% probability level. The hydrogen atoms are omitted for clarity. Dashed lines represent hydrogen bonds.

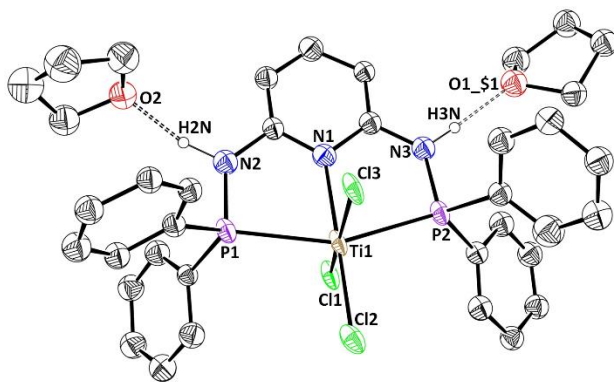


Figure 4 – Structural view of complex (4) [Ti(PNP-Ph₂)Cl₃] showing thermal ellipsoids at 40% probability level. The hydrogen atoms are omitted for clarity.

The geometries around the vanadium^{III} and titanium^{III} metal centres are best described as distorted octahedral. The three meridionally placed donor atoms of the PNP ligand and one chlorine atom occupy the equatorial plane of the octahedron. In all complexes the P-M-Cl angles are higher than 90° while the N-M-P bond angles are significantly more contracted (less than 90°) towards the pyridine ring. The other two chlorine atoms occupy the axial positions with the Cl-M-Cl (M=V,Ti) angles significantly deviated from linearity, attesting the octahedral distortion. In all structures, the M-P(1) bond and the M-P(2) bond distances are similar, except for **2** and **4** which show a length difference of 0.0280 and 0.0342 Å. This occurrence may be due to the stereochemical constraint inflicted by the phenyl substituents.

Two different solvomorph structures of [V(PNP-*i*Pr₂)Cl₃] were obtained. Using a CH₂Cl₂/toluene system led to the formation of **1a** that displays a co-crystallized molecule of CH₂Cl₂ (Figure 1A), occupying the voids of the supramolecular network. On the other hand, the THF/toluene system provided **1b** that contains two co-crystallized THF (Figure 1B). In **1a** two bond interactions of the type N-H...Cl between the amino spacers and the chlorine atoms are observed with distances of 2.585 and 2.433 Å. In **1b** a co-crystallized THF molecule is hydrogen bonded to one amino group of the PNP ligand while the other displays a hydrogen bond with a chlorine atom from a neighbor molecule. Once more, the disposition to form solvates is exhibited in the isostructural complexes **2** and **4**. In both cases, two THF molecules interact with the NH spacers of the PNP ligand by hydrogen bonds of the type N-H...O.

It is plausible that the stereochemical constrain created by the presence of the phenyl groups affects the formation of this type of structure, blocking the interaction with parent molecules, as observed in **1a** and **1b**. The absence of N-H groups in [V(PNP^{Me-i}Pr₂)Cl₃] may justify the lack of co-crystallized solvent molecules in this compound.

Table II - Selected bond lengths (Å) and angles (°) of the compounds [V(PNPⁱPr₂)Cl₃] (1), [V(PNPPH₂)Cl₃] (2), [V(PNP^{Me-i}Pr₂)Cl₃] (3) and [Ti(PNP-Ph₂)Cl₃] (4)

	1a	1b1	1b2	2	3a1	3a2	4
M-N(1)	2.140(5)	2.152(5)	2.159(4)	2.173(2)	2.152(2)	2.156(1)	2.22(1)
M-P(1)	2.494(2)	2.500(2)	2.470(2)	2.4738(7)	2.4758(7)	2.4776(6)	2.576(6)
M-P(2)	2.480(2)	2.501(2)	2.476(2)	2.5080(7)	2.4767(7)	2.4703(7)	2.548(5)
M-Cl(1)	2.366(2)	2.302(2)	2.390(2)	2.3098(7)	2.3284(6)	2.3280(6)	2.323(5)
M-Cl(2)	2.320(2)	2.286(2)	2.285(2)	2.2810(7)	2.2856(6)	2.3041(7)	2.365(6)
M-Cl(3)	2.301(2)	2.378(2)	2.286(2)	2.3261(7)	2.3527(6)	2.3197(6)	2.338(5)
P(1)-M-N(1)	79.6(2)	78.82(15)	79.83(15)	79.09(5)	79.62(5)	79.65(5)	76.7(4)
P(2)-M-N(1)	80.6(2)	79.49(15)	79.55(15)	78.48(5)	79.47(5)	80.00(5)	78.1(4)
P(1)-M-Cl(2)	100.65(8)	101.52(7)	99.34(7)	100.84(2)	100.90(2)	100.05(2)	102.48(19)
P(2)-M-Cl(2)	99.22(8)	100.19(7)	101.16(7)	101.62(3)	100.00(2)	100.22(2)	101.82(19)
Cl(1)-M-Cl(3)	171.38(8)	171.07(7)	168.11(7)	168.59(3)	172.17(3)	168.15(2)	168.7(2)

Table II - Bond lengths (Å) for the intermolecular bondings.

	1a	1b1	1b2	2	4
N-H...O	-	2.037	2.026	2.083 2.062	1.948 1.946
N-H...Cl	2.585 2.433	2.632	2.812	-	-

3. Concluding Remarks

The synthesis of early metal^{III} complexes based on PNP ligands of formulas $[V(\text{PNP-}^i\text{Pr}_2)\text{Cl}_3]$, $[V(\text{PNP-Ph}_2)\text{Cl}_3]$, $[V(\text{PNP}^{\text{Me},i}\text{Pr}_2)\text{Cl}_3]$, $[\text{Ti}(\text{PNP-Ph}_2)\text{Cl}_3]$ and $[\text{Y}(\text{PNP-Ph}_2)\text{Cl}_2][\text{YCl}_4]$ are described. Titanium and yttrium PNP pincer complexes were not reported before. The synthesis of all complexes was accomplished by treatment of $\text{MCl}_3(\text{THF})_3$ ($\text{M}=\text{V}$ and Ti) and $\text{YCl}_{3.5}(\text{THF})_{3.5}$ with the respective PNP ligand. The solid state molecular structures of all V^{III} and Ti^{III} complexes were determined by single crystal X-ray diffraction showing octahedral geometries.

4. Experimental Section

General Procedures

Unless otherwise stated, all manipulations were performed under an atmosphere of dry oxygen-free nitrogen by means of standard Schlenk and glovebox techniques.

Solvents were pre-dried using 4 Å molecular sieves and refluxed over sodium-benzophenone (Et_2O , toluene and THF), CaH_2 (*n*-hexane, dichloromethane), P_2O_5 (acetonitrile) or sodium (methanol) under an atmosphere of N_2 , and collected by distillation. The compounds $(\text{THF})_3\text{VCl}_3$ ^[5], $(\text{THF})_3\text{TiCl}_3$ ^[6] and $(\text{THF})_{3.5}\text{YCl}_3$ ^[7] were prepared according to previously described procedures. 2,6-diaminopyridine was purified by stirring the crude product over active charcoal in a solution of dichloromethane followed by filtration and solvent evaporation. All other reagents were commercial grade and used without further purification.

Infrared spectra were recorded on a Jasco FT/IR – 410 spectrometer using KBr as support and on a Perkin-Elmer 400 FIR FTIR spectrometer, equipped

with a Pike Technologies GladiATR using a diamond crystal plate at TU-Wien.

Elemental analyses were obtained using a Fisons Instruments Mod. EA-1108, from Laboratório de Análises do IST, Lisbon, Portugal. All samples were sent in glass ampules sealed under nitrogen atmosphere.

Mass spectra (ESI-MS) were recorded on a Varian 500-MS ion trap mass spectrometer with nitrogen as the nebulizer gas at 35.0 psi, drying gas at 350°C and 15.0 psi, capillary voltage of 80.0 and needle voltage of +5000 V.

Magnetic susceptibility measurements as function of Evan's Method were performed with a capillary with acetone as solvent in a BRUKER AVANCE 250 MHz and 300 MHz spectrometer at 296 K, referenced internally to residual proton-solvent (^1H) resonances and reported relative to tetramethylsilane (0 ppm).

Crystals suitable for single-crystal X-ray analysis were grown as described in the synthetic procedures. Crystals of air/moisture sensitive compounds were selected inside the glovebox, covered with polyfluoroether oil and mounted on a nylon loop. The data were collected using a graphite monochromated Mo- $\text{K}\alpha$ radiation ($\lambda = 0.71073 \text{ \AA}$) on a BRUKER AXS-KAPPA APEX II diffractometer equipped with an Oxford Cryosystem open-flow nitrogen cryostat. Cell parameters were retrieved using Bruker SMART software and refined using Bruker SAINT on all reflections. Absorption corrections were applied using SADABS^[8]. The structures were solved and refined using direct methods using SIR92^[9], SIR97^[10], SIR2004^[11]. Structure refinement was done using SHELXL-97^[12]. These programs are part of the WinGX software package version 1.80.01^[13]. Torsion angles, mean square planes and other geometrical parameters

were calculated using SHELX^[14]. Unless stated otherwise, all non-hydrogen atoms were refined anisotropically and the hydrogen atoms were inserted in idealized positions and allowed to refine riding on the parent carbon atom. Illustrations of the molecular structures were made with ORTEP-3 for Windows^[15].

N,N'-Bis(diisopropylphosphino)-2,6-diaminopyridine (PNP-*i*Pr₂) A ^[1,d]

Triethylamine (2.64 mL, 18.86 mmol) was added to a suspension of 2,6-diaminopyridine (1.029g, 9.43 mmol) in toluene (100 mL). The mixture was cooled at 0°C and P(*i*Pr)₂Cl (3 mL, 18.86 mmol) was added dropwise. The solution was allowed to reach room temperature and was refluxed overnight. The reaction mixture was then filtered and the solvent was removed under vacuum to give an yellow oil. If necessary (NMR analysis of ³¹P) the obtained oil can be purified to give a white crystalline solid **A** by flash chromatography, using silica gel (conditioned with 5 Vol% NEt₃) and 3:1 PE/EE, with EE as the eluent.

Yield: 2.62 g (81%) white crystalline solid; C₁₇H₃₃N₃P₂ (MW: 341.42); 59.81% C, 9.74% H, 12.31% N, 18.14% P.

¹H NMR (δ, CDCl₃, 20 °C): 7.23 (t, J = 8.1 Hz, 1H, py⁴), 6.42 (dd, J = 8.0 Hz, J = 2.1, 2H, py^{3,5}), 4.48 (d, J = 10.7 Hz, H, NH), 1.72 (m, J = 7.0 Hz, J = 1.9 Hz, 4H, CH(CH)₃)₂, 1.07-0.97 (m, 24H, CH(CH₃)₂)

IR (cm⁻¹): 3340, (m.); 2950 (m.); 2865 (m.); 1582 (s.); 1444 (s.); 1384 (m.); 1347 (m.); 1278 (m.); 1245 (m.); 1148 (m.); 1099 (w.); 1079 (w.); 1012 (m.); 922 (w.); 878 (m.); 795 (m.); 780 (m.); 729 (m.); 664 (m.); 619 (m.); 567 (m.); 480 (m.); 441 (w.); 419 (w.).

N,N'-Bis(diphenylphosphino)-2,6-diaminopyridine (PNP-Ph) B ^[1,d]

This ligand was prepared analogously to **A** with NEt₃ (5.1 mL, 36.65 mmol), 2,6-diaminopyridine (2g,

18.33mmol) and P(Ph)₂Cl (7.2 mL, 36.65 mmol) as starting materials. The obtained white solid **B** can be purified, if necessary (NMR analysis of ³¹P), by flash chromatography, using silica gel (conditioned with 5 Vol% NEt₃) and 1:1:1 PE/EE/DCM, with EE as the eluent.

Yield: 7.11 g (81%) white solid; C₂₉H₂₅N₃P₂ (MW: 477.49); 72.95% C, 5.28% H, 8.80% N, 12.97% P.

¹H NMR (δ, CDCl₃, 20 °C): 7.46-7.36 (m, 21H, Ph, py⁴), 6.53 (dd, J = 7.9 Hz, J = 1.2, 2H, py^{3,5}), 5.47 (d, J = 8.2 Hz, 2H, NH);

IR (cm⁻¹): 3215 (m.); 3070 (w.); 3055 (w.); 1953 (w.); 1881 (w.); 1805 (w.); 1645 (m.); 1598 (s.); 1575 (s.); 1501 (m.); 1481 (m.); 1445 (vs.); 1431 (s.); 1348 (m.); 1304 (w.); 1260 (s.); 1179 (w.); 1153 (m.); 1092 (m.); 1025 (s.); 998 (w.); 907 (w.); 843 (w.); 807 (m.); 783 (m.); 736 (s.); 694 (s.); 604 (m.); 557 (m.); 512 (s.); 474 (m.); 443 (m.); 427 (m.).

Complex 1: [V(PNP-*i*Pr₂)Cl₃]

To a suspension of (THF)₃V(Cl)₃ (892.55 mg, 2.41 mmol) in THF, PNP-*i*Pr (822.30 mg, 2.41 mmol) was added. The reaction mixture was stirred for 2 hours at room temperature. The solvent was then removed under vacuum. The remaining brown solid was washed twice with toluene (10 mL) and twice with Et₂O (10 mL) and finally dried under vacuum. Crystals suitable for single crystal x-ray diffraction were obtained from diffusion of a THF solution into Toluene.

Yield: 867.30 mg (72%) brown solid; C₁₇H₃₃Cl₃N₃P₂V (MW: 498.71);

IR (cm⁻¹): 3304 (vs.); 3060 (w.); 2963 (s.); 2930 (s.); 2872 (s.); 1613 (vs.); 1578 (s.); 1569 (s.); 1457 (vs.); 1398 (s.); 1369 (s.); 1290 (m.); 1254 (m.); 1203 (m.); 1167 (s.); 1102 (s.); 1065 (s.); 1028 (s.); 931 (m.); 884 (vs.); 841 (s.); 783 (s.); 736 (m.); 673 (s.);

603 (m.); 569 (m.); 529 (m.); 475 (m.); 444 (m.), 412 (w.).

ESI-MS (m/z): ESI (-) = 532/534/536/538 [V(PNP-*i*Pr)Cl₄]⁻; 495/498/499/500 [V(PNP⁺⁺-*i*Pr₂)Cl₃]⁻;

ESI (+) = 443/445/446 [V(PNP-*i*Pr₂)ClO]⁺; 462/464 [V(PNP-*i*Pr₂)Cl₂]⁺;

Elemental Analysis calculated for C₁₇H₃₃Cl₃N₃P₂V (%): N = 8.43, C = 40.94, H = 6.67.

Found: N = 7.81, C = 42.56, H = 7.31.

Complex 2: [V(PNP-Ph₂)Cl₃]

To a suspension of (THF)₃V(Cl)₃ (1.55g, 4.19 mmol) in THF, PNP- PNP-Ph (2g, 4.19 mmol) was added. After the reaction mixture was stirred for 2 hours at room temperature, the precipitate formed was filtered off and the solvent was removed under vacuum. The remaining green solid was washed twice with toluene (10 mL) and twice with Et₂O (10 mL) and finally dried under vacuum. Crystals suitable for single crystal x-ray diffraction were obtained from diffusion of a THF solution into Toluene.

Yield: 1.60g (60%) green solid; C₂₉H₂₅Cl₃N₃P₂V (MW: 634.78);

IR (cm⁻¹): 3278 (s.); 3177 (s.); 3054 (s.); 2974 (s.); 2915 (s.); 2875 (s.); 1964 (w.); 1891 (w.); 1815 (w.); 1611 (vs.); 1577 (vs.); 1456 (vs.); 1436 (vs.); 1391 (s.); 1332 (m.); 1298 (m.); 1209 (m.); 1169 (s.); 1103 (vs.); 1040 (vs.); 998 (s.); 894 (s.); 854 (s.); 789 (s.); 735 (s.); 695 (s.); 632 (m.); 582 (m.); 521 (vs.); 484 (s.); 404 (w.).

ESI-MS (m/z): ESI (-) = 667/669/671/672 [V(PNP-Ph)Cl₄]⁻; 632/634/636 [V(PNP⁺⁺-Ph₂)Cl₃]⁻;

ESI (+) = 579/581 [V(PNP-Ph₂)ClO]⁺;

Elemental Analysis calculated for C₂₉H₂₅Cl₃N₃P₂V (%): N = 6.62, C = 54.87, H = 3.97.

Found: N = 5.68, C = 56.88, H = 4.56.

Complex 3: [V(PNP^{Me}-*i*Pr)Cl₃]

This complex was prepared analogously to **1** with (THF)₃V(Cl)₃ (402.3 mg, 1.09 mmol) and PNP^{Me}-*i*Pr (400 mg, 1.09 mmol) as starting materials. Crystals suitable for single crystal x-ray diffraction were obtained from diffusion of Et₂O into a THF solution.

Yield: 389 mg (68%) green solid; C₁₉H₃₇Cl₃N₃P₂V (MW: 526.77);

IR (cm⁻¹): 2965 (w.); 2928 (w.); 2873 (w.); 1649 (s.); 1449 (vs.); 1417 (s.); 1387 (w.); 1370 (w.); 1344 (w.); 1286 (s.); 1286 (w.); 1243 (m.); 1193 (m.); 1164 (m.); 1137 (m.); 944 (m.); 856 (s.); 779 (s.); 733 (s.); 666 (m.); 633 (w.)

Complex 4: [Ti(PNP-Ph₂)Cl₃]

This complex was prepared analogously to **1** with (THF)₃Ti(Cl)₃ (174.9 mg, 4.76 mmol), PNP- PNP-Ph (250 mg, 5.24 mmol) as starting materials, with the exception that the reaction mixture was refluxed overnight at 90°C. Crystals suitable for single crystal x-ray diffraction were obtained from diffusion of a THF solution into Toluene.

Yield: 162 mg (54%) brown solid; C₂₉H₂₅Cl₃N₃P₂Ti (MW: 631.70);

IR (cm⁻¹): 3051 (m.); 2966 (m.); 2871 (m.); 1961 (w.); 1890 (w.); 1814 (w.); 1645 (s.); 1616 (s.); 1577 (s.); 1458 (s.); 1435 (s.); 1394 (m.); 1295 (m.); 1262 (m.); 1167 (m.); 1102 (m.); 1067 (m.); 1036 (m.); 1026 (m.); 997 (m.); 897 (m.); 858 (m.); 793 (m.); 742 (s.); 691 (vs.); 557 (m.); 518 (s.); 480 (m.).

ESI-MS (m/z): ESI(-) = 662/663/665/667/669 [Ti(PNP-Ph)Cl₄]⁻;

Elemental Analysis calculated for C₂₉H₂₅Cl₃N₃P₂Ti (%): N = 3.99, C = 55.14, H = 6.65.

Found: N = 4.90, C = 54.04, H = 4.75.

Complex 5: [Y(PNP-Ph)Cl₂]YCl₄

This complex was prepared analogously to 1 with (THF)₃Y_{3.5}(Cl)₃ (372.7 mg, 8.38 mmol), PNP- PNP-Ph (200 mg, 4.19 mmol) as starting materials, with the exception that the reaction mixture was refluxed overnight at 90°C.

Yield: 91 mg (34%) white solid; C₂₉H₂₅Cl₆N₃P₂Y₂ (MW: 868);

IR (cm⁻¹): 3388 (vs.); 1961 (w.); 1893 (w.); 1822.4 (w.); 1639 (s.); 1480 (w.); 1449 (m.); 1434 (m.); 1395 (w.); 1355 (w.); 1295 (w.); 1262 (w.); 1166 (m.); 1094 (m.); 1070 (w.); 1026 (w.); 997 (w.); 818 (w.); 741 (m.); 695 (m.); 558 (w.); 514 (w.); 484 (w.);

Elemental Analysis calculated for C₂₉H₂₅Cl₆N₃P₂Y₂ (%): N = 4.84, C = 40.13, H = 2.90.

Found: N = 4.40, C = 36.65, H = 3.84.

5. Bibliography

- [1] (a) Albrecht, M.; van Koten, G. *Angew. Chem. Int. Ed.* 2001, 40, 3750. (b) Van der Boom, M. E.; Milstein D. *Chem. Rev.* 2003, 103, 1759. (c) Wanniarachchi, S., *The Impact of Ligand Design on the Coordination Chemistry and Reactivity of metal pincer complexes*; 2009, Marquette University. (d) Benito-Garagorri, D.; Becker, E.; Wiedermann, J.; Lackner, W.; Pollak, M.; Mereiter, K.; Kisala, J.; Kirchner, K., *Organometallics* 2006, 25 (8), 1900-1913.
- [2] (a) Morales-Morales, D.; Pincer complexes. *Applications in Catalysis*; *Rev. Soc. Quím. Méx.* 2004, 48, 338-346. (b) Yoon, M.; Ryu, D.; Kim, J, Ahn, K. H. *Organometallics*, 2006, 25, 2409–2411. (c) Kozlov, L. A.; Aleksanyan, D. V.; Nelyubina, Y. V.; Lyssenko, K. A.; Petrovskii, P. V.; Vasil'ev, A. A.; Odinets, I. L. *Organometallics*, 2011, 30, 2920–2932. (d) G Suzuki, A. J. *Organomet. Chem.* 1999, 576, 147–168. (e) Baumann, R.; Davis, W. M.; Schrock, R. R. J., *Am. Chem. Soc.* 1997, 119, 3830. (f) Naota, T.; Takaya, H.; Murahashi, S.-I., *Chem. Rev.* 1998, 98, 2599. (g) Bedford, R. B.; Draper, S. M.; Scully, P. N.; Welch, S. L. *New J., Chem.* 2000, 24, 745–747. (h) 14 Ohff, M.; Ohff, A.; van der Boom, M. E.; Milstein, D. J., *Am. Chem. Soc.* 1997, 119, 11687–11688.
- [3] (a) Evans, D. F.; *J. Chem. Soc.* 1959, 36, 2003. (b) Evans, D. F.; Fazakerley, G. V.; Phillips, R. F., *J. Chem. Soc.* 1971, A, 1931. (c) Evans, D. F.; Jakubovic, D. A., *J. Chem. Soc., Dalton Trans.* 1988, 2927. (d) Grant, D. H., *J. Chem. Educ.* 1995, 72, 39.
- [4] (a) Bichler, B.; Glatz, M.; Stöger, B.; Mereiter, K.; Veiros, L.F.; Kirchner, K.; *Dalton Transactions*, 43, 2014, S. 14517 - 14519. (b) Glatz, M.; Bichler, B.; Mastalir, M.; Stöger, B.; Weil, M.; Mereiter, K.; Pittenauer, E.; Allmaier, G.; Veiros, L.F.; Kirchner, K., *Dalton Transactions*, 44, 2015, S. 281 - 294.
- [5] Manzer, L.E. *Inorg. Synth.* 1982, 21, 135.
- [6] Jones, N.A.; Liddle, S. T.; Wilson, C.; Arnold, P. L. *Organometallics* 2007, 26, 755.
- [7] den Haan, K.H.; de Boer, J.L.; Teuben, J.H.; Spek, A.L.; Kojic-Prodic, B.; Hays, G.R.; Huis, R. *Organometallics* 1986, 5, 1726.
- [8] Sheldrick, G.M.; *SADABS, Program for Empirical Absortion Corrections*; University of Göttingen: Göttingen, Germany, 1996.
- [9] Altomare, A.; Cascarano, G.; Giacovazzo C.; Guagliardi, A., *J. Appl.Crystallogr.*, 1993, 26, 343-350.
- [10] Altomare, A.; Burla, M.C.; Camalli, M.; Cascarano, G.L.; Giacovazzo, C.; Guagliardi, A.; Moliterni, A.G.G.; Polidori, G.; Spagna, R., *J. Appl.Crystallogr.*, 1999, 32, 115.
- [11] Burla, M.C.; Caliendo, R.; Camalli, M.; Carozzini, B.; Cascarano, G.L.; De Caro, L.; Giacovazzo, C.; Polidori, G.; Spagna, R., *J. Appl.Crystallogr.*, 2005, 38, 381.
- [12] Sheldick, G.M.; *Acta Crystallographica Section A. Foundations of Crystallography.*, 2008, 64, S112-S122
- [13] Sheldick, G.M.; *Acta Crystallographica Section A. Foundations of Crystallography.*, 2008, 64, S112-S122.
- [14] Farrugia, L.J.; *J. Appl.Crystallogr.*, 1999, 32, 837.
- [15] Farrugia, L.J.; *J. Appl.Crystallogr.*, 1997, 30, 565.

6. Acknowledgments

Prof. Dr. Ana Margarida Martins is gratefully acknowledged for being my supervisor and allowing me to develop my masters' thesis in her laboratories. I also thank Prof. Dr. Karl Kirchner for accepting me as a transfer student and for allowing me to learn the basis of this work subject in his laboratories. To both, my special thanks for the support during the whole work.